Adsorbed States of Phosphonate Derivatives of N-Heterocyclic Aromatic Compounds, Imidazole, Thiazole, and Pyridine on Colloidal Silver: Comparison with a Silver Electrode

ARTICLE *in* THE JOURNAL OF PHYSICAL CHEMISTRY B · SEPTEMBER 2009

Impact Factor: 3.3 · DOI: 10.1021/jp9050116 · Source: PubMed

Adsorbed States of Phosphonate Derivatives of *N*-Heterocyclic Aromatic Compounds, Imidazole, Thiazole, and Pyridine on Colloidal Silver: Comparison with a Silver Electrode

Edyta Podstawka,*,† Tomasz K. Olszewski,‡ Bogdan Boduszek,‡ and Leonard M. Proniewicz§

Regional Laboratory of Physicochemical Analysis and Structural Research, Faculty of Chemistry, Jagiellonian University, ul. Ingardena 3, 30-060 Krakow, Poland, Organic Chemistry Division, Faculty of Chemistry, Wroclaw University of Technology, ul. Wybrzeże S. Wyspiańskiego 27, 50-370 Wrocław, Poland, and Faculty of Chemistry, Jagiellonian University, ul. Ingardena 3, 30-060 Krakow, Poland

Received: May 28, 2009; Revised Manuscript Received: July 17, 2009

Here, we report a systematic surface-enhanced Raman spectroscopy (SERS) study of the structures of phosphonate derivatives of the *N*-heterocyclic aromatic compounds imidazole (**ImMeP** ([hydroxy(1H-imidazol-5-yl)methyl]phosphonic acid) and **$(ImMe)_2P$** (bis[hydroxy-(1H-imidazol-4-yl)-methyl]phosphinic acid)), thiazole (**BAThMeP** (butylaminothiazol-2-yl-methyl)phosphonic acid) and **BzAThMeP** (benzylaminothiazol-2-yl-methyl)phosphonic acid)), and pyridine (**$(PyMe)_2P$** (bis[(hydroxypyridin-3-yl-methyl)]phosphinic acid)) adsorbed on nanometer-sized colloidal particles. We compared these structures to those on a roughened silver electrode surface to determine the relationship between the adsorption strength and the geometry. For example, we showed that all of these biomolecules interact with the colloidal surface through aromatic rings. However, for **BzAThMeP**, a preferential interaction between the benzene ring and the colloidal silver surface is observed more so than that between the thiazole ring and this substrate. The PC(OH)C fragment does not take part in the adsorption process, and the phosphonate moiety of **ImMeP** and **$(ImMe)_2P$**, being removed from the surface, only assists in this process.

Introduction

Proteases or peptidases are enzymes that catalyze reactions on peptide chains, hydrolyzing them into short fragments by splitting the peptide bond between amino acid residues located either within the ribbon (endopeptidases) or at the polymeric backbone end (exopeptidases). These enzymes can be further categorized according to the reactant groups that are present in the catalytic site, as with the serine (EC 3.4.21), cysteine (EC 3.4.22), aspartic acid (EC 3.4.23), and metallo (EC 3.4.24) proteases. Their control over protein synthesis, turnover, and function enables them to regulate physiological processes such as digestion, fertilization, growth, differentiation, cell signaling/migration, immunological defense, wound healing, and apoptosis.[1−5] Proteases of these classes are also crucial for disease propagation, and inhibitors of such proteases are emerging as promising therapeutics in the treatment of diseases.[6−9]

Trypsin-like enzymes, a group of serine proteases, are causative or adjunctive in many disease states. The hyperproteolytic activities of this homologous family of enzymes make them attractive chemotherapeutic targets in pathways of blood coagulation, fibrinolysis, kinin formation, complement activation, digestion, reproduction, and phagocytosis.[10,11] Inhibitors of this class of serine proteases could, in principle, remedy many disease states, and therefore, several classes of compounds have been designed and synthesized as potential inhibitors of this group of enzymes. It has been well established that molecules composed of phosphorus moieties (especially phosphonate diphenyl esters, $P(O)(OPh)_2$) linked to peptides are a class of very potent transition-state inhibitors of trypsin-like proteases.[12−16] The reaction of trypsin with those inhibitors to form a tetrahedral adduct is thought to proceed via an associative pathway. The transition state of this reaction contains a trigonal bipyramidal, pentacoordinated phosphorus atom with donor and acceptor ligands in apical positions. Phosphonylation of the active serine, in the catalytic site, results in an immediate loss of one phenoxy group. The second phenoxy group appears to be hydrolyzed during the aging of the phosphonylated derivative.[17−19]

Due to the presence of the phosphorus moiety in the phosphorylated derivatives of pyridine, imidazole, and thiazole presented here, we have decided to investigate their inhibitory activity toward proteases. Preliminary tests were performed on chymotrypsin from bovine pancreas, and they revealed only moderate activity of the tested compounds (12−25% inhibition).[20] According to the data in the literature, it appears that the replacement of the phosphonic acid moiety ($-PO_3H_2$) in the tested compounds with the phosphonate diphenyl ester functionality ($-P(O)(OPh)_2$) should improve their inhibitory activity.

In order to gather more evidence explaining the contribution of the structural features of the aforementioned phosphorylated heterocyclic derivatives on their ability to interact with the potential receptor, we have decided to undertake careful investigative work using spectroscopic techniques. We recently provided a systematic study of the surface-enhanced Raman scattering (SERS) characteristics of several phosphonic (**ImMeP** ([hydroxy(1H-imidazol-5-yl)methyl]phosphonic acid), **BAThMeP** ((butylamino-thiazol-2-yl-methyl)phosphonic acid), and **BzAThMeP** ((benzylaminothiazol-2-yl-methyl)phosphonic acid) and phosphinic (**$(ImMe)_2P$** (bis[hydroxy(1H-imidazol-4-yl)methyl]phosphinic acid) and **$(PyMe)_2P$** (bis[(hydroxypyridin-3-yl-methyl)]phosphinic acid)) acids (see Table 1 for their molecular structures) deposited onto the surface of an electro-

* To whom correspondence should be addressed. E-mail: podstawk@chemia.uj.edu.pl. Phone: +48-12-663-2077. Fax: +48-12-634-0515.
† Regional Laboratory of Physicochemical Analysis and Structural Research, Faculty of Chemistry, Jagiellonian University.
‡ Wroclaw University of Technology.
§ Faculty of Chemistry, Jagiellonian University.

10.1021/jp9050116 CCC: $40.75
Published on Web 08/11/2009

chemically roughened silver electrode.[21] In this work, our interest was centered on a silver surface since silver exhibits a very large enhancement factor over a wide range of excitation wavelengths and is an active catalyst for a number of important reactions. Hence, we correlated the contribution of the structural components of these biomolecules to their inhibitory ability toward chymotrypsin from bovine pancreas using the SERS patterns. We also showed that the adsorption process on this surface mainly occurs through the N lone pair of electrons of imidazole (Im), thiazole (Th), and pyridine (Py), with the ring arranged in a largely edge-on manner for **ImMeP** and **BzAThMeP** and in a slightly inclined orientation to the silver electrode surface for **(ImMe)$_2$P**, **BAThMeP**, and **(PyMe)$_2$P**. We propose the formation of a localized C═C bond, which is accompanied by a decrease in the ring−surface π-electron overlap for **ImMeP** and **(PyMe)$_2$P** and a Bz/Ag complex for **BzAThMeP**. We also suggest an interaction of a phosphonate group with the strength of the P═O coordination to the silver electrode, which was highest for **ImMeP** and lowest for **BzAThMeP**. However, for a proper understanding of the SERS spectra, a reliable assignment of all of the vibrational bands is essential. Therefore, we performed a vibrational spectroscopic characterization of the nonadsorbed molecular structures of these compounds.[22] In this study, we present the equilibrium geometries for the ground state and those relevant for biomolecules consisting of zero to five bonded water molecules. This work also provides the definitive band assignments needed to generate vibrational spectra useful for a structural analysis primarily based on DFT (density functional theory) calculations at the B3LYP, 6-31++G** level using Gaussian03 software. Our aim was to produce an extensive look-up table of Raman spectra that could make the structural determination of these biomolecules a rapid and accurate process.

In order to verify the proposed importance of the Im, Th, Py, and Bz rings and the phosphonate group for both the surface coordination and receptor affinity, in the present paper, we carried out SERS characterizations of the aforementioned biomolecules adsorbed on a colloidal silver surface. We analyzed, in detail, the orientation of the species on this surface and the surface bond and further compared these results with those for a silver electrode surface. Finally, we rationalized the difference between the adsorption schemes on the colloidal and silver electrode surfaces. These differences result from changes in the type of metal roughness (size/shape/aggregation) and charge because the morphology of the metallic nanostructures is a primary factor determining the sensitivity of the detection, the magnitude of the signal enhancement, and the surface geometry of the analytes.[23,24] These effects are of great importance in the context of nanobiomedicine, protein screening, and other therapeutic applications and, hence, should be fully understood. Therefore, we used the SERS technique to obtain further insight into the possible ways in which these biomolecules interact with the surrounding medium, such as how they bind to their receptors. This was done because the observed biomolecule−nanoparticle aggregates provide, by nature of their geometry, a unique and unprecedented opportunity to probe a biomolecule−nanoparticle interface at the molecular level and to obtain specific information about molecular conformational changes occurring at that interface.[25−29] Thus, we provide missing structural information concerning the chemisorption of these biomolecules on silver surfaces.

Experimental Section

Synthesis of Heterocyclic Phosphonic Acids. The phosphonic acids **ImMeP**, **BAThMeP**, and **BzAThMeP** and the phosphinic acids **(ImMe)$_2$P** and **(PyMe)$_2$P** used in this study were synthesized according to a previously described procedure.[30,31] The purity and chemical structures of these samples were proven by means of ^{1}H,^{31}P, and ^{13}C NMR spectra (Bruker Avance DRX 300 MHz spectrometer) and electrospray mass spectrometry.

SERS Measurements. $AgNO_3$ and $NaBH_4$ were purchased from Sigma−Aldrich Co. (Poznan, Poland) and used without further purification. Three batches of colloidal silver solution were prepared according to standard procedures.[32] Briefly, 8.5 mg of $AgNO_3$ dissolved in 50 mL of deionized water at 4 °C was added dropwise to 150 mL of 1 mM $NaBH_4$ and immersed in an ice bath while the mixture was stirred vigorously. After the $AgNO_3$ was added, the resulting pale yellow solution was stirred continuously at 4 °C for approximately 1 h. The excitation spectra of three batches of the Ag solution prepared in this manner showed an absorbance maximum at 396 nm.

We have masterd the above method for years in order to get reproducible silver colloidal particles (the same surface organization, thus the same binding affinity) from experiment to experiment.

Aqueous sample solutions were prepared by dissolving the samples in deionized water. The concentration of the samples before mixing with the colloids was adjusted to 10^{-4} M. The freshly prepared sample solution was added to the silver solution such that the final sample concentration in the silver colloid solution was $\sim 10^{-5}$ M. The final pH was 8.3.

The SERS spectra of the investigated molecules were collected twice using each batch of the three silver colloids with a triple-grating spectrometer (Jobin Yvon, T 64000) equipped with a liquid-nitrogen-cooled CCD detector (Jobin Yvon, model CCD3000). The spectral resolution was set at 4 cm^{-1}. The 514.1 nm line of an Ar ion laser (Spectra−Physics, model 2025) was used as an excitation source. The laser power at the sample was set at 20 mW ($\sim$0.5 W/cm^2).

All of the SERS spectra were recorded within 1 h of adding the sample to the Ag solution. The spectra obtained were almost identical, except for small differences (up to $\sim$5%) in some band intensities. No spectral changes that could be associated with sample decomposition or desorption processes were observed during these measurements.

Results and Discussion

The curves of Figure 1 are the SERS spectra, taken using an Ar ion laser at 514.5 nm, of the investigated biomolecules adsorbed on the colloidal silver surface. For comparison, the curves of Figure 2 illustrate the respective normal Raman spectra in a neat solid state. In general, these SERS spectra (Figure 1) are more similar to the Raman spectra (Figure 2), considering both the spectral pattern and the relative band intensities, than the corresponding SERS spectra of these species immobilized on the silver electrode surface.[21] It can also clearly be seen that the SERS spectral pattern in the silver sol is different from that on the silver electrode.[21] The most noteworthy points are that the strong spectral features due to the ν_{19a} and PC(OH)C deformation motions and the two medium-strong bands assignable to higher- and lower-wavenumber P═O stretching identified at $\sim$1501, $\sim$1396, 1268, and 1142 cm^{-1}, respectively, in the SERS spectra of these species immobilized on the silver electrode surface almost disappear in the SERS spectra on the silver nanoparticles (Figure 1); however, the ν(P═O) modes could be slightly identified at around 1268 and 1148 cm^{-1} for **ImMeP** and **(ImMe)$_2$P** on the silver nanoparticles. In addition, a

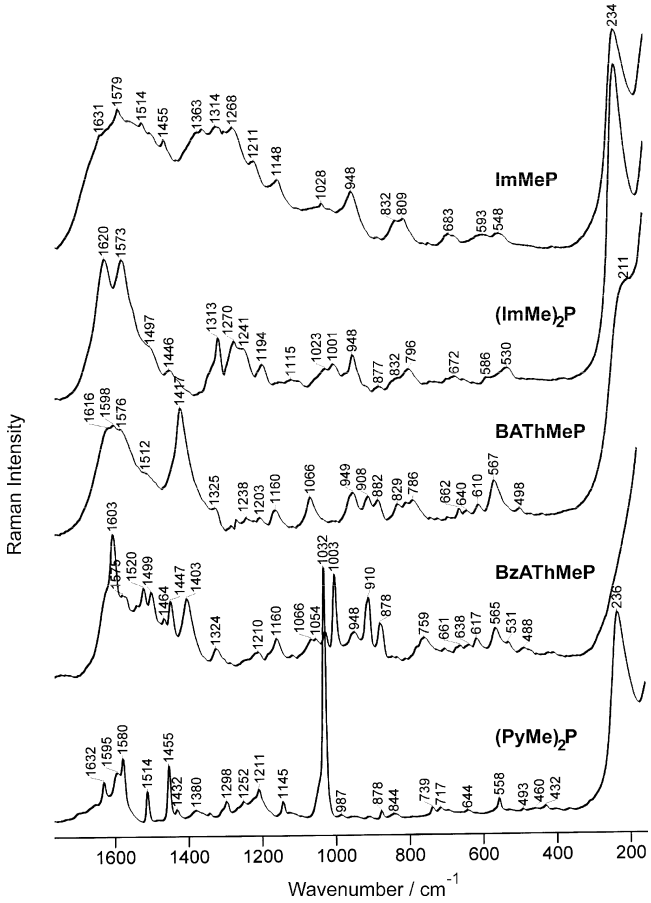

Figure 1. SERS spectra of **ImMeP**, **(ImMe)$_2$P**, **BAThMeP**, **BzAThMeP**, and **(PyMe)$_2$P** adsorbed on a colloidal silver surface in the spectral range of 1700−150 cm^{-1}.

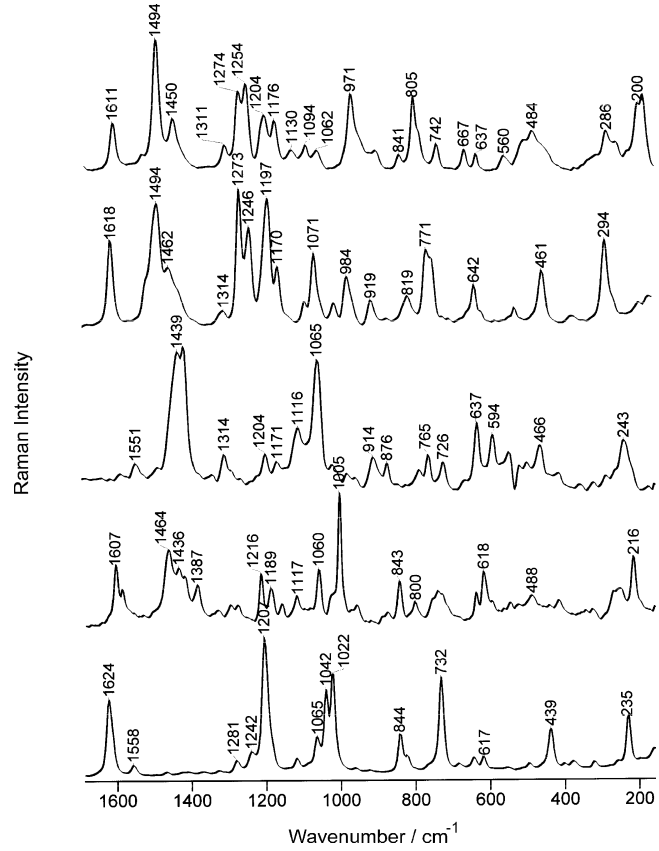

Figure 2. RS spectra of **ImMeP**, **(ImMe)$_2$P**, **BAThMeP**, **BzAThMeP**, and **(PyMe)$_2$P** in the spectral range of 1700−150 cm^{-1}.

marked decrease in the enhancement of the δ/ρ_b(PC(N)C) band (1403 cm^{-1}) is obvious for **BzAThMeP** on the colloidal surface of silver. Similar observations were made for the ∼1002 cm^{-1} band of **ImMeP**, **(ImMe)$_2$P**, and **BAThMeP** on the silver electrode. On the other hand, it was found that this band of **BzAThMeP** in the silver sol is not much more intense than that measured on the silver electrode, whereas the band of the Py trigonal ring breathing vibration (1032 cm^{-1}) of **(PyMe)$_2$P** in the silver sol is several times more enhanced than that on the silver electrode (1034 cm^{-1}). These observed changes, and the changes described below, are related to the alternative interaction of the aromatic rings and the phosphonate fragment of these biomolecules with each of the silver surfaces, as is typical of complexes of these biomolecules with metals.[30,31] To discuss these spectral alterations due to the different surface adsorption mechanisms of these biomolecules, the spectral changes must be analyzed according to the adsorption process. Hence, a correct vibrational assignment is required in this respect. Consulting the previously published allocation to the normal mode motions for the Raman and SERS spectra of imidazole,[33,34] thiazole,[35,36] pyridine,[37,38] and benzene,[39] as well as the phosphonate derivatives of small peptides,[40,41] in Table 2, we propose and summarize the appropriate SERS assignments along with the band positions observed in the SERS spectra in the silver sol. The latter assignments are taken from our earlier reports.[21,22]

Almost all of the spectral features in the SERS spectrum of **(PyMe)$_2$P** (Figure 1, bottom trace) could be correlated, without difficulty, to the Py ring vibrations, except for the weakest bands assignable to the vibrations of the phosphinic group. These include the SERS signals at 1632, 1595, 1580, 1514, 1380, 1298, 1211, 1145, 1032, 739, and 644 cm^{-1} (see Table 2 for the band assignments) that closely correspond to the bands reported by Johnson and Soper for Py adsorbed on silver nanoparticles in a citrate sol.[38] They also are in good agreement with those previously observed in Py SERS spectra in colloidal solutions[42,43] and with those for **(PyMe)$_2$P** immobilized on a roughened silver electrode.[21] Therefore, we conclude that **(PyMe)$_2$P** interacts with both of the silver substrates mainly through Py. As mentioned earlier, the major differences in the enhancement between the colloidal and electrode **(PyMe)$_2$P** SERS spectra are the stronger scattering at 1032 cm^{-1} and the weaker or lack of scattering at 1380 (δ/ρ_b(PC(OH)C)), ∼1273 (ν(P═O)), and 1134 cm^{-1} (ν(P═O)) in the silver sol. The fact that a more marked shift in the wavenumber of the Py SERS bands is observed in the silver sol (Figure 1, bottom trace), as compared to the silver electrode,[21] is also noteworthy; for example, $\nu_1 + \nu_{6b}$ moves by 8 and −1 cm^{-1}, ν_{9a} by 4 and 0 cm^{-1}, ν_{12} by −10 and −8 cm^{-1}, and ν_1 by −35 and −15 cm^{-1} on the nanoparticle and electrode surfaces, respectively. In general, the slightly higher shifts and the relative intensity enhancement observed for the bands attributed to the Py ring as well as the weakening of the phosphinic group bands in sol, compared to the electrode, indicate that **(PyMe)$_2$P** interacts with the colloidal silver mainly through Py (slightly stronger for the nanoparticle surface than for the electrode surface), leading to a specific orientation in which the Py ring is oriented vertically to this surface and the phosphinic group is located further from the surface.

A similar conclusion regarding the phosphonate group interactions with the silver nanoparticle surfaces can be made for **BzAThMeP** and **BAThMeP** adsorbed on the colloidal silver. In their SERS spectra, the bands due to the ν(P−OH), ν(C−P), or ρ_b(P−OH) (see Table 2 for the band positions) modes are only negligibly enhanced, whereas the two bands due to the P═O bond

TABLE 1: Molecular Structures of ImMeP, $(ImMe)_2P$, BAThMeP, BzAThMeP, and $(PyMe)_2P$

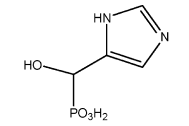

ImMeP
[Hydroxy-(1H-imidazol-5-yl)-methyl]-phosphonic acid

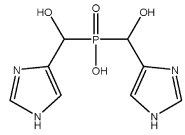

$(ImMe)_2P$
Bis-[hydroxy-(1H-imidazol-4-yl)-methyl]-phosphinic acid

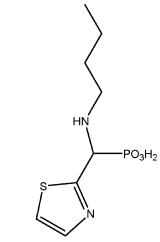

BAThMeP
(Butylamino-thiazol-2-yl-methyl)-phosphonic acid

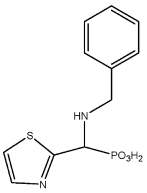

BzAThMeP
(Benzylamino-thiazol-2-yl-methyl)-phosphonic acid

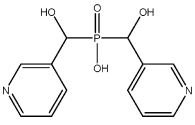

$(PyMe)_2P$
Bis-[(hydroxy-pyridin-3-yl-methyl)]-phosphinic acid

vibrations are absent. This is contrary to the results obtained for these biomolecules immobilized on the electrode surface, which show that the oxygen electron lone pairs of the P═O moiety assist in the interaction with the electrode surface. On the other hand, it seems that the benzene ring in a tilted orientation preferentially interacts, with moderate strength, with both the electrode and colloidal silver surfaces. However, the tilt angle with respect to the surface normal is smaller in the sol than that with the electrode surface. This conclusion is made based on the strong enhancement of the SERS signals at 1603, 1568, 1499, 1464, and 1003 cm^{-1} (Figure 1) and the intensification of the 1003 cm^{-1} band in the sol. Furthermore, the slightly higher wavenumber shifts of the Bz ring modes observed in the SERS spectrum of **BzAThMeP** in the sol (up to 18 cm^{-1}) in comparison to those in the SERS spectrum at the roughened electrode (by 1−12 cm^{-1}) are indicative of the formation of a slightly stronger Bz···Ag complex in the sol than that on the electrode. In addition, a 910 cm^{-1} band due to C−C stretching gained relative intensity, which may indicate that the C−C bond adjacent to the benzene ring is in close contact with the silver nanoparticles. This contact is probably accompanied by a conformational change of either the PCN(H)C fragment or the thiazole ring, which reduces the strength of interaction between the nitrogen lone pair of electrons and the colloidal silver surface, as deduced from the decrease in the relative intensity of the 1403 cm^{-1} band (ρ_b(PCN(H)C) and/or ν(C═N)$_{Th}$) in relation to the same band in the SERS spectra of **BzAThMeP** deposited on the roughened silver electrode. On the other hand, the 1417 cm^{-1} SERS signal dominates the SERS spectrum of **BAThMeP** adsorbed on the colloidal silver surface, similar to the case of the electrode surface, and is as intense as that in the SERS spectrum of this biomolecule deposited on the roughened silver electrode. It is also broad (fwhm = 41 cm^{-1}, full width at half-maximum) and asymmetric. Hence, it probably overlaps with the band assignable to the other Th ring vibrations. These facts must be considered as evidence of direct interactions between the nitrogen lone pair of electrons and the silver nanoparticles.

Considering the other thiazole ring modes, a few trends can be noted in their SERS spectral profiles. First, many of the same Th modes are enhanced in the SERS spectra of **BzAThMeP** and **BAThMeP** adsorbed on the colloidal silver (see Table 2). However, some significant differences between the SERS spectra of **BAThMeP** on the colloidal silver and the roughened silver electrode surfaces are observed. These dissimilarities are connected to the Th ν_7 and ν_9 modes, which appear at 1239 and 1007 cm^{-1} in the SERS spectrum on the electrode and are absent in the SERS spectrum measured in the sol. Second, the positions of the Th bands coincide within a few wavenumbers in the SERS spectra of both biomolecules adsorbed on the silver nanoparticles (see Table 2). However, the relative intensities of the Th bands are negligibly higher for **BAThMeP** in the sol than those for **BzAThMeP** on the same substrate. On the basis of the above results, we deduced that the thiazole rings of **BzAThMeP** and **BAThMeP** interact with the colloidal silver nanoparticles in a horizontal orientation with respect to the surface; although, for **BzAThMeP**, the thiazole ring is slightly farther from the surface than that in the case of **BAThMeP**.

The influence of the silver substrate substitution on the behavior of **ImMeP** and **$(ImMe)_2P$** is also evident. For instance, the most intensified spectral features at 1396, 1240, and 1006 cm^{-1} in the **$(ImMe)_2P$** SERS spectrum on the electrode are replaced by the bands at 1620 and 1573 cm^{-1}, due to C_4═C_5 stretching, in the SERS spectrum of this biomolecule in the silver sol. Thus, the colloidal silver surface induces a preferential, edge-on conformation of the Im ring of **$(ImMe)_2P$** for which two N_1 and N_3 tautomers are present. This fact can be supported by the observation of several weak SERS signals assignable to the in-plane imidazole ring modes, that is, 1543, 1497, 1446, 1313, 1241, and 1194 cm^{-1} (see Table 2 for the band allocations). The wavenumber shifts of these modes on both silver substrates are comparable. Thus, the strength of the Im···Ag interactions is similar on both of the substrates. Similarly, the position of the higher-wavenumber ν(P═O) mode and the relative intensity remain almost invariant in the spectra on the colloidal and electrode surfaces, suggesting that the oxygen atom lone pair of electrons forms a complex of similar strength with both silver substrates. In this way, we observed that the adsorption through the oxygen atom of the PC(OH)C group is no longer possible on the nanoparticle surface, which is demonstrated by the lack of the 1396 cm^{-1} band that is enhanced in the **$(ImMe)_2P$** SERS spectrum on the roughened silver electrode.

In the case of **ImMeP**, the different complex mainly affects the bands appearing at 1501, 1268, 1142, and 1002 cm^{-1}. The very strong SERS signals at 1501 and 1002 cm^{-1}, allocated to the in-plane Im motion in the **ImMeP** SERS spectrum on the roughened silver electrode, are almost diminished in the spectrum of this molecule adsorbed on the colloidal silver surface. Generally, a trend of a decrease in the enhancement of the bands due to the in-plane Im ring modes is observed for this substrate, whereas an increase in the relative intensity of the 948 and 832 cm^{-1} bands (out-of-plane) is detected (see Table 2 for the band allocations). According to the SERS selection rules,[44−46] a selective enhancement of the out-of-plane vibrational modes over the in-plane modes of the adsorbed **ImMeP** indicates that the Im ring is oriented in a flat-on manner to the surface. Two other highly pronounced bands at 1268 and 1142 cm^{-1} also undergo a remarkable decrease in the relative intensity in the SERS spectrum in the sol. However, the positions of these bands in both of the SERS spectra coincide within 0 and 4 cm^{-1},

Publication Date (Web): August 11, 2009 | doi: 10.1021/jp9050116

TABLE 2: Wavenumbers and Proposed Band Assignments for the SERS Spectra of ImMeP, $(ImMe)_2P$, BAThMeP, BzAThMeP, and $(PyMe)_2P$ Adsorbed on a Colloidal Silver Surface[a]

wavenumbers [cm^{-1}]			wavenumbers [cm^{-1}]			wavenumbers [cm^{-1}]		
ImMeP	**$(ImMe)_2P$**	literature assignment fo Im[b]	**BAThMeP**	**BzAThMeP**	literature assignment for Th and Bz[c]	**$(PyMe)_2P$**	literature assignment for Py[d]	assignment B3LYP/6-311*[e]
	1620	$\nu_{ip}(C_4{=}C_5)_{Im}$ (taut N_3) $\nu(C^{+}N) + \nu(CN)$				1632		
1579	1573	$\nu_{ip}(C_4{=}C_5)_{Im}$ (taut N_1)	1598	1603	Bz/Th (ν_{8a}, A_1)	1595	ν_{8a} [ν(Py)], A_1	
				1575				
1514	1543	$\nu_{ip}(C_2N_1 + C_5N_1)_{Im} + \rho_{inb}(N{-}H)$	1576	1568	Bz/Th (ν_{8b}, B_2)	1580	ν_{8b}[ν(Py)], B_2	
				1540				
1493	1497	$\nu_{ip}(C_2N_3 + C_4N_3 + C_5N_1)_{Im} + \rho_{inb}(C_2{-}H)$	1512	1520	Bz/Th (ν_{19a}, A_1)	1514	semicircle ν_{19a} [δ(CH)$_{Py}$], A_1 or $2\nu_4$, A_1	$\rho_r(C{-}H)_\phi + \nu(C{-}C)_\phi + \nu(C{-}N)_\phi$, $\rho_r(N{-}H) + \rho_s(CH_2)$
				1499				
				1464	Th (ν_4, A′), Bz (ν_{19b}, B_2)			$\rho_r(C{-}H)_{Bz} + \nu(C{-}C)_{Bz}$
1455	1446	ν_{ip}(Im) + $\delta(N_1H)$		1447		1455	ν_{19b} [δ(CH)$_{Py}$], B_2	$\rho_r(C{-}H)_\phi + \nu(C{-}C)_\phi + \nu(C{-}N)_\phi$
			1417	1403	Th (ν_5 [ν(C═N)], A′)	1380		δ(PC(H)C)), ρ_b(C−OH), δ/ρ_b(PC(−O)C), ρ_b(CNHC), ρ_w(CH)
1363			1325		Th (ν_6 [ρ_r(CH) + ν(C═N)], A′), Bz (ν_3, B_2)	1345	ν_{14} [δ(CH)$_{Py}$], B_2	$\rho_r(C{-}H)_\phi + \nu(C{-}N)_\phi + \rho_r(C{-}H)$, ρ_b(C−OH), $\rho_w(CH_2)$, $\nu(C{-}C)_{Bz}$
1352	1339[f]	ρ_b(CH)						$\nu(C{-}N)_{Im} + \nu(C{-}C)_{Im} + \rho_t(C{-}H)$
1314	1313	$\nu_{ip}(Im)_{breathing}$		1324	Bz (ν_4, B_2)	1298	$2\nu_{6b}$, A_1	$\delta(CH_3)$, $\rho_r(C{-}H) + \rho_b$(C−OH) + $\nu(C{-}N)_\phi + \rho_r(C{-}H)_\phi$, $\rho_t(CH_2) + \rho_w(CH_2) + \rho_r(C{-}H)_{Th} + \rho_r(C{-}H)$
1268	1270	δ(Im), $\rho_{inb}(C_2H)$	1267					ν(P═O)
	1241	$\nu_{ip}(Im)_{breathing}$	1238		Th (ν_7 [ρ_w(CH)], A′)	1252	ν_3 [δ(CH)$_{Py}$], B_2	$\rho_r(C{-}H)_{Th} + \nu(C{-}C)_{Th}$ and/or $\rho_r(C{-}H)$, $\rho_t(CH_2)$, $\rho_r(CH_2)$, $\delta(CH_3)$, ρ_b(CNH)
1211	1194	δ(Im)	1203	1210	Bz (ν_{7a}, A_1)	1211	ν_{9a} [ν(Py)], A_1	ν(P−O) + ρ_b(P−OH) + ρ_r(C−H), $\rho_r(C{-}H)_{Im}$
1146		$\nu_{ip}(C_5N_1)_{Im}$	1160	1160	Bz ($\nu_{9a/15}$, A_1/B_1), Th (ν_8 [ρ_r(CH)], A′)	1145		ν(P═O), $\delta(CH_3)$
	1094	$\rho_{ipb}(C_5H)$						$\nu(C{-}N)_{Im} + \rho_r(C{-}H)_{Im}$
			1066	1066	Bz (ν_{18b}, B_2)			$\nu(C{-}C)_\phi + \delta(\phi)$, $\nu(C{-}S)_{Th}$, ν(C−N), ρ_b(CNC), δ(PCC)
				1054				
1028	1001	$\rho_{ip}(CH)_{Im}$		1003	Th (ν_9 [ρ_r(CH)], A′) Bz (ν_{12}, A_1)	1032	ν_{12} [$\nu(Py)_{trig.breath}$], A_1	
				1027	Bz (ν_{18a}, A_1)			
						987	ν_1 [$\nu(Py)_{totally\ sym.breeth}$], A_1	
948	948	γ_{oop}(CH), δ(Im)	948	948	Bz ($\nu_{5/17a}$, B_1/A_2)			$\rho_r(CH_2) + \rho_t(CH_2) + \delta(CH_3)$, ν(C−N), ρ_b(P−OH), ν(P−O) + ν(C−P)
			908	910				ν(C−C)
	877	ρ_{ipb}(Im), ν(CC)	882	878	Th ($\nu_{10/11}$ [δ(Th)], A′)	878		ν(P−O) + ν(C−P), ρ_b(P−OH), ν(C−C)
832	832	$\rho_{oopb}(CH)_{Im}$	829		Th (ν_{14}, A″), Bz (ν_{10a}, A_2)	844		$\rho_w(C{-}H) + \nu(P{-}O) + \rho_b(P{-}OH) + \nu(C{-}P)$
809	796	$\nu(Im)_{breathing}$	807		Th (ν_{15}, A″; ρ_w(CH))			$\rho_w(C{-}H)_\phi + \delta_{oop}(\phi)$, ν_{as}(OPO)
			786	759	Th (ν_{12}, A′)			$\rho_r(CH_2)_{Th}$, δ_{oop}(Bz) + $\rho_w(C{-}H) + \rho_w(C{-}H)_{Bz}$, $\nu(C{-}P) + \rho_s$(CCP), ν_s(OPO)
						739		$\rho_w(C{-}H)_{Im} + \delta_{oop}$(Im) + ρ_b(CCP) + ν(P−O) + ν(C−C)
						717	ν_4 [ρ_t(Py)], B_1	
683	672	γ_{oopb}(Im)	662	661				$\nu(C{-}P) + \delta_{oop}(\phi) + \rho_b$(PCO) + ν(P−O), ρ_{tors}(P−OH)
			640	638		644	ν_{6b} [δ(Py)], B_2	$\delta_{oop}(\phi) + \rho_b$(CCP) + ρ_b(CCO), ρ_w(CPO), $\delta_{as}(PO_2H)$
593	586	ρ_{oopb}(Im)	610	617	Th (ν_{17}, A″) Bz (ν_{6b}, B_2)			
548	530		567	565	Bz (ν_{16b}, B_1)	558		$\delta_{oop}(\phi)$, ρ_b(CCP) + ρ_b(CCO) + $\delta(PO_2)$, $\delta_{as}(PO_2H)$, ρ_b(CPO)
				531				
			498	488		493		$\rho_w(PO_2) + \rho_b$(PCO)
234	234	ν(Ag molecule)	211	192	ν(Ag molecule)	236	ν(Ag molecule)	

[a] Abbreviations: Im, imidazole; Th, thiazole; Bz, benzyl; Py, pyridine rings; ϕ, aromatic ring; ν, stretching; δ, deformation; ρ_w, wagging; ρ_b, bending; ρ_t, twisting; ρ_r, rocking; ρ_s, scissoring; A″ or oop, out of plane; A′ or ip, out of plane vibrations; γ, torsion. [b] Assignment made on the basis of refs 33 and 34. [c] Assignment made on the basis of refs 35, 36, and 39. [d] Assignment made on the basis of refs 37 and 38. [e] Assignment made on the basis of refs 21 and 22. [f] Shoulder.

respectively, whereas they are down-shifted in wavenumber by 5 cm^{-1} in comparison to those in the **ImMeP** Raman spectrum. This indicates that the oxygen atom of the P═O moiety does not directly interact with both substrates, which, in the case of the silver nanoparticle surface, is removed far from this surface.

Conclusions

The structures of five phosphonate derivatives of *N*-heterocyclic aromatic compounds (imidazole (**ImMeP** and **$(ImMe)_2P$**), thiazole (**BAThMeP** and **BzAThMeP**), and pyridine (**$(PyMe)_2P$**)) adsorbed on nanometer-sized colloidal particles were investigated by SERS. These structures were compared with the adsorption geometries of these same molecules adsorbed on a roughened silver electrode. By observing the band shift in wavenumbers, the bandwidth broadening, and the enhancement changes in the vibrational modes of the aromatic ring, PC(O/N)C, and the phosphonate moieties in the SERS spectra, we made the following conclusions:

(i) The adsorption process on both the electrode and colloidal silver surfaces mainly occurs through the N lone pair of electrons of imidazole (Im), thiazole (Th), and pyridine (Py); however, in the case of **BzAThMeP**, it seems that the benzene ring in a edge-on orientation preferentially interacts (slightly stronger in the sol than on the electrode) with both of these substrates with the tilt angle with respect to the surface normal smaller in the sol than that with the electrode.

(ii) The C−C bond adjacent to the benzene ring is in close contact only with the silver nanoparticle surface; this contact probably reduces the strength of interaction between the nitrogen lone pair of electrons and the colloidal silver surface.

(iii) The Py ring of **$(PyMe)_2P$** interacts slightly stronger with the nanoparticle surface than with the electrode surface; on the latter surface, the Py ring is slightly inclined, whereas it is oriented vertically to the silver nanoparticle surface.

(iv) The Th ring of **BzAThMeP** and **BAThMeP** interacts with the colloidal silver surface in a flat-on orientation with respect to the surface; although, for **BzAThMeP**, the thiazole ring is slightly farther from the surface than that in the case of **BAThMeP**. This is contrary to the results on the silver electrode surface that show that the Th ring of **BzAThMeP** and **BAThMeP** is arranged in a largely edge-on manner and in a slightly inclined orientation to this substrate, respectively.

(v) The colloidal silver surface induces a preferential, edge-on conformation of the Im ring of **$(ImMe)_2P$** (a slightly inclined orientation to the silver electrode surface).

(vi) The Im ring of **ImMeP** is oriented in a flat-on and edge-on manner to the colloidal silver and electrode surfaces, respectively.

(vii) The phosphonate group of **ImMeP** and **$(ImMe)_2P$** only assists in the adsorption process on the colloidal silver surface, while it plays an important role in the adsorption process on the electrochemically roughened silver electrode for all investigated molecules.

(viii) The adsorption through the oxygen atom of the PC(OH)C group is not possible on the nanoparticle surface.

Acknowledgment. This work was supported by the Polish State Department for Scientific Research (Grant No. N N204 159136 to E.P.).

References and Notes

(1) Babine, R. E.; Bender, S. L. *Chem. Rev.* **1997**, *97*, 1359.
(2) Ripka, A. S.; Rich, D. H. *Curr. Opin. Chem. Biol.* **1998**, *2*, 441.
(3) Craik, M. S.; Debouck, C. Proteases as Therapeutic Targets. In *Perspectives in Drug Discovery and Design*; McKerrow, J. H., James, M. N. G., Eds.; ESCOM: Leiden, The Netherlands, 1995; Vol. 2, pp 1−125.
(4) Shaw, E. *Adv. Enzymol. Relat. Areas Mol. Biol.* **1990**, *63*, 271.
(5) Leung, D.; Abbenante, G.; Fairlie, D. P. *J. Med. Chem.* **2000**, *43*, 305.
(6) Yan, S.; Sameni, M.; Sloane, B. F. *Biol. Chem.* **1998**, *379*, 113.
(7) Brindley, P. J.; Kalinna, B. H.; Dalton, J. P.; Day, S. R.; Wong, J. W.; Smythe, M. L.; McManus, D. P. Proteolytic degradation of host hemoglobin by schistosomes. *Mol. Biochem. Parasitol.* **1997**, *89*, 1.
(8) Li, Z.; Chen, X.; Davidson, E.; Zwang, O.; Mendis, C.; Ring, C. S.; Roush, W. R.; Fegley, G.; Li, R.; Rosenthal, P. J. *Chem. Biol.* **1994**, *1*, 31.
(9) West, M. L.; Fairlie, D. P. *Trends Pharmacol. Sci.* **1995**, *16*, 67.
(10) Beynon, R. J., Bond J. S., Eds. *Proteolytic Enzymes: A Practical Approach*; Oxford University: Liverpool, U.K., 1989.
(11) Neurath, H. *Science* **1984**, *224*, 350.
(12) Lambden, L. A.; Bartlett, P. A. *Biochem. Biophys. Res. Commun.* **1983**, *112*, 1085.
(13) Bartlett, P. A.; Lambden, L. A. *Bioorg. Chem.* **1986**, *14*, 356.
(14) Sampson, N. S.; Bartlett, P. A. *Biochemistry* **1991**, *30*, 2255.
(15) Oleksyszyn, J.; Powers, J. C. *Biochemistry* **1991**, *30*, 485.
(16) Oleksyszyn, J.; Boduszek, B.; Kam, C.; Powers, J. C. *J. Med. Chem.* **1994**, *37*, 226.
(17) Bone, R.; Sampson, N. S.; Bartlett, P. A.; Agard, D. A. *Biochemistry* **1991**, *30*, 2263.
(18) Oleksyszyn, J.; Powers, J. C. *Methods Enzymol.* **1994**, *244*, 423.
(19) Bertrand, J. A.; Oleksyszyn, J.; Kam, Ch.-M.; Boduszek, B.; Presnell, S.; Plaskon, R. R.; Suddath, F. L.; Powers, J. C.; Williams, L. D. *Biochemistry* **1996**, *35*, 31473155.
(20) (a) Unpublished results; part of Olszewski, T. Ph.D. Thesis, Wroclaw University of Technology, Poland, 2006. (b) The biological assays were performed according to the literature methodology; see: Sienczyk, M.; Oleksyszyn, J. *Bioorg. Med. Chem. Lett.* **2006**, *16*, 2886 (inhibitor concentration 23 μM; chymotripsin concentration 1.29 μM).
(21) Podstawka, E.; Kudelski, A.; Olszewski, T. K.; Boduszek, B. *J. Phys. Chem. B* **2009**, *113*, 10035.
(22) Andrzejak, M.; Podstawka, E.; Boduszek, B.; Olszewski, T. K.; Proniewicz, L. M. *J. Phys. Chem. B.* To be submitted.
(23) Kneipp, K.; Kneipp, H.; Itzkan, I.; Dasari, R. R.; Feld, M. S. *Chem. Rev.* **1999**, *99*, 2957.
(24) Pettinger, B.; Wenning, U.; Kolb, D. M. *Ber. Bunsen-Ges. Phys. Chem.* **1978**, *82*, 1326.
(25) Podstawka, E.; Kudelski, A.; Kafarski, P.; Proniewicz, L. M. *Surf. Sci.* **2007**, *601*, 4586.
(26) Podstawka, E.; Kudelski, A.; Proniewicz, L. M. *Surf. Sci.* **2007**, *601*, 4971.
(27) Podstawka, E. *Biopolymers* **2008**, *89*, 980.
(28) Podstawka, E.; Ozaki, Y.; Proniewicz, L. M. *Langmuir* **2008**, *24*, 10807.
(29) Podstawka, E.; Kafarski, P.; Proniewicz, L. M. *J. Phys. Chem. A* **2008**, *112*, 11744.
(30) Olszewski, T. K.; Boduszek, B.; Sobek, S.; Kozłowski, H. *Tetrahedron* **2006**, *62*, 2183.
(31) Podstawka, E.; Proniewicz, L. M. *J. Phys. Chem. B* **2009**, *113*, 4978.
(32) Markham, L. M.; Mayne, L. C.; Hudson, B. S.; Zgierski, M. Z. *J. Phys. Chem.* **1993**, *97*, 10319.
(33) Cao, P.; Gu, R.; Tian, Z. *J. Phys. Chem.* **2003**, *107*, 769.
(34) Hegelund, F.; Wugt Larsen, R.; Palmer, M. H. *J. Mol. Struct.* **2007**, *244*, 63.
(35) Palmer, M. H. *J. Mol. Struct.* **2007**, *834−836*, 113.
(36) Zuo, Ch.; Jagodziński, P. W. *J. Phys. Chem. B* **2005**, *109*, 1788.
(37) Johnson, C. K.; Soper, S. A. *J. Phys. Chem.* **1989**, *93*, 7281.
(38) Podstawka, E.; Drag, M.; Oleksyszyn, J. *J. Raman Spectrosc.* **2009**, *40*, doi: 10.1002/jrs.2299.
(39) Podstawka, E.; Kudelski, A.; Drag, M.; Oleksyszyn, J.; Proniewicz, L. M. *J. Raman Spectrosc.* **2009**, *40*, doi: 10.1002/jrs.2301.
(40) Podstawka, E.; Kudelski, Proniewicz, L. M. *Surf. Sci.* **2007**, *601*, 4971.
(41) Creighton, J. A.; Blatchford, C. G.; Albrecht, M. G. *J. Chem. Soc., Faraday Trans. 2* **1979**, *75*, 790.
(42) Lippitch, M. E. *Chem. Phys. Lett.* **1980**, *74*, 125.
(43) Pemberton, J. E.; Carter, D. A. *Langmuir* **1992**, *8*, 1218.
(44) Campion, A.; Kambhamapati, P. *Chem. Soc. Rev.* **1998**, *27*, 241.
(45) Creighton, J. A. In *Spectroscopy of surfaces*; Clark, R. J., Hester, R. E., Eds.; Wiley: New York, 1998; Chapter 2.
(46) Lombardi, J. R.; Birke, R. L. *J. Phys. Chem. C* **2008**, *112*, 5605.

JP9050116